Percolation Transitions in the Hard-Sphere Fluid

Leslie V. Woodcock
Dept. of Chemical Engineering, Colburn Laboratory, University of Delaware, Newark, DE 19716

DOI 10.1002/aic.12666
Published online May 23, 2011 in Wiley Online Library (wileyonlinelibrary.com).

*The number densities (*N/V*) above or below which "pockets" of additional-sphere excluded volume (ρ_{pe}) and available volume (ρ_{pa}) begin to percolate the whole volume of the system, sometimes referred to as percolation thresholds, have been determined for the equilibrium hard-sphere fluid of diameter σ using a Monte Carlo (MC) approach. Values obtained are $\rho_{pe}\sigma^3 = 0.0785 \pm 0.01$ and $\rho_{pa}\sigma^3 = 0.537 \pm 0.005$. The present value of $\rho_{pe}\sigma^3$ agrees with an interpolation of previous data for the percolation diameter (σ_p) for various densities from Heyes et al. The available volume (*V_a*) can be resolved as a "radial acceptance function" (u(r)), which is easily obtained from MC acceptance ratio statistics providing a direct route to the chemical potential up to liquid-like densities. The closed-virial equation-of-state of the hard-sphere fluid is found to deviate slightly, but significantly from thermodynamic pressures at densities exceeding ρ_{pa}. Knowledge of the hard-sphere fluid percolation transitions could lead to a more formal description of the critical point and origins of the liquid state, in the spirit of van der Waals.* © 2011 American Institute of Chemical Engineers *AIChE J,* 58: 1610–1618, 2012

Keywords: thermodynamics/classical, thermodynamics/statistical, simulation, molecular, percolation transition

Introduction

Ever since van der Waals published his theory on the equation-of-state of gases and liquids,[1] based on excluded volume of two spheres, the hard-sphere fluid has played an abiding role in the development of liquid-state theory. van der Waals was able to obtain an equation-of-state resembling gases and liquids and coexistence, by simply adding an attractive mean field, proportional to the square of density, to an "excluded volume" hard-sphere equation-of-state for the thermodynamic pressure of N spheres of diameter σ in volume V at temperature T.

$$Z_{\rm vw} = \frac{V}{(V - Nb_2)} = \sum_{n=0}^{\infty} (b_2\ \rho)^n \tag{1}$$

Here, Z is $pV/(Nk_BT)$, ρ is the number density $N\sigma^3/V$, and $b_2 = 2\ \pi\sigma^3/3$. The constant b_2 represents an excluded volume (V_e/N) based only on collision of only two spheres. The corresponding accessible volume is the complement of V_e, i.e., $V_a = (V - Nb_2)$. When van der Waals hard-sphere equation (Eq. 1) is expanded in powers of density and compared with the exact low-density virial expansion of gases from the cluster theory of Mayer,[2]

$$Z = \sum_{n=1}^{\infty} b_n \rho^{(n-1)} \tag{2}$$

only the first two terms of van der Waals hard-sphere equation are correct in describing the exact virial equation-of-state at low density. Virial coefficients beyond $n = 2$ depend on the

Correspondence concerning this article should be addressed to L. V. Woodcock at les.woodcock@manchester.ac.uk.

size of the cluster n. b_n can then be computed[2,3] by integrating over all space, the excluded volumes of clusters of spheres of size n. Modern theories of simple liquids[3] are based on the assumption that the thermodynamic hard-sphere fluid equation-of-state can be represented by Eq. 2, i.e., by an expansion based on the excluded volume of small clusters.

The correct expression for the excluded volume, which takes account of all many-body correlations in a dense fluid and which gives the chemical potential and hence also corrects equation-of-state for a system of N hard spheres, was derived by Hoover and Poirier.[4] They considered the potential of mean force $\Psi(r)$ between two hard spheres in the equilibrium fluid as a function of separation (r). At zero separation, $\Psi(0)$ relates to the chemical potential, and for hard-spheres defines a "thermodynamic" excluded volume (V_e), which defines the available volume $V_a = (1 - V_e)$. For any equilibrium thermodynamic state, the available volume can be defined as the volume available for relocation of any one sphere i, anywhere in an equilibrium configuration, and is exactly related to the excess chemical potential (μ), relative to the ideal gas at the same T and V for large N according to

$$-\frac{\mu}{k_B T} = \log_e \frac{Q_{N-1}}{Q_N} = \log_e\left(1 - \frac{<V_e>}{V}\right) = \log_e \frac{<V_a>}{V} =_{\mathrm{Lt}.\rho->0} \sum_{n=1}^{\infty} \frac{(n+1)}{n} b_{(n+1)} \rho^n \quad (3)$$

The Mayer cluster theory (Eq. 3) is strictly only rigorous for thermodynamic properties at low density.[2] Nonetheless, it is widely assumed in liquid-state theory to represent the thermodynamic state functions over the whole equilibrium fluid range up to high liquid densities.[3]

Hoover and Poirier's equation for hard spheres was generalized by Widom[5] to continuous pair potential Hamiltonians, and has since become a standard method for calculating the chemical potential in computer simulations of all molecular fluids. Knowledge of the available volume directly provides the chemical potential according to Eq. 3. The first such computations for hard spheres are described in the article by Adams[6] 35 years ago. These exact expressions, for the available and excluded free volumes, and the numerical computational means to compute these quantities have been known for many years, yet essential properties have hitherto remained undetermined. It is well known,[7–11] for instance, that all hard-core fluids undergo percolation transitions in V_a and V_e as functions of state, which could be of importance in understanding not only the liquid state[12,13] but also both the linear and nonlinear transport properties of colloidal fluids.[14]

The percolation transition for the excluded volume V_e occurs at the density below which the overlapping exclusion spheres of diameter 2σ form clusters of size small n with size $n = 1$ being the most likely, and above which clusters of order size N span the whole system, which at liquid densities is just one single cluster. The percolation transition for the available volume is the density above which V_a comprises a distribution in configuration space of accessible holes, i.e., with no other sphere center within distance of one sphere diameter. Following Kratky, we will designate the percolation transition densities of available and excluded volumes as ρ_{pe} and ρ_{pa}, respectively, but here preferring subscripts. (Note that Kratky uses ρ for the packing fraction: $\pi/6 \times N\sigma^3/V$.)

Percolation transitions are easier to describe and understand in two dimensions (Figure 1) than in three dimensions.[7] The available volume percolation transition was determined from Monte Carlo (MC) studies by Hoover et al.[8] for the two-dimensional system of hard disks; they obtained a value for the percolation density $\rho_{pa}\sigma^2 = 0.4$. For hard disks, the percolation of excluded volume coincides with the percolation of available volume; i.e., for $D = 2$ $\rho_{pe} = \rho_{pa}$, this is not the case when $D = 3$.

For spheres, there are two percolation transitions associated with the excluded and available volumes. The V_a-percolation transition can equally be defined as the density at which the mean "accessible" configurational integral of a single sphere in the static field of all j (sometimes referred to as "Hoover's free volume" V_f), within the equilibrium ensemble, changes from being extensive at low density to intensive at high density. Above the percolation density ρ_{pa}, only the available volume in the immediate vicinity of sphere i is "accessible." There is an inequality for spheres[11] $\rho_{pe} < \rho_{pa}$.

For densities below the accessible percolation density $\rho < \rho_{pa}$, $V_a = V_f$ and both are extensive. In the density range $\rho_{pe} < \rho < \rho_{pa}$, the available volume for an additional sphere remains a network of diffusive pathways to the whole system, until, at the density ρ_{pa} it becomes a distribution of disconnected discrete "holes" which are accessible only to an incoming sphere, but not accessible by diffusion of sphere i in an equilibrium configuration when all the remaining j are fixed. Above ρ_{pa}, the mean single sphere accessible free volume $<V_f>$ becomes intensive as one mobile sphere is trapped in its own cavity, whereas V_a remains an extensive distribution of discrete "holes."

The first evidence for identification of the percolation transition with a thermodynamic phase transition was found in a molecular dynamics (MD) study of hard parallel cubes.[9] The percolation transition in a free volume coincides with a weak discontinuity in transport coefficients as functions of state and with a deviation of the virial equation-of-state from the thermodynamic pressure at percolation. Kratky[11] using scaling arguments gave rough estimates of percolation transitions in hard spheres, which he discussed, in his searching paper, with the title question "Is the percolation transition of hard spheres a thermodynamic phase transition." From the current results and analyses, it appears that the answer to Kratky's question is "yes"; however, for spheres, is it at ρ_{pe} or ρ_{pa} or, indeed, both?

Excluded Volume Percolation

A detailed generalized determination of the values of the hard-sphere percolation threshold diameter (σ_p) as a function of all densities has been reported by Heyes et al.[15]

It appears that these authors were unaware of the earlier work[11–13] and did not see the special theoretical significance of $\sigma_p = 2$. This can easily be obtained, however, by interpolation between the neighboring packing fractions ($y = 0.0325$ and 0.05, corresponding to $r = 0.07162$ and 0.09549, respectively). In this region, parameterizing the data given in Table 1 of Ref. 15, one obtains the relationship $\sigma_p =$

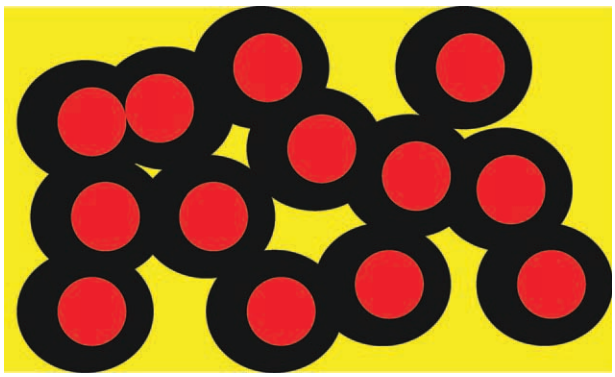

Figure 1. Two-dimensional illustration of available volume (V_a: yellow) and excluded volume (V_e: red plus black).

If σ is the diameter of the spheres, the radius σ from the center of red spheres defines the excluded volume and available volume; the total volume $V = V_a + V_e$. [Color figure can be viewed in the online issue, which is available at wileyonlinelibrary.com.]

$0.5828\rho^{(-2.9183)}$ from which we obtain a value of $\rho_{pe} = 0.0711$ with uncertain error bounds.

Here, we investigate the percolation transition density, ρ_e, directly by a completely different approach and begin by defining a state function $n_c(\rho)$ that is the total number of clusters of any size n, normalized to 1 at $\rho = 0$ whereupon $n_c = n$ and all clusters are of size 1 sphere. A cluster of size n is simply defined as a group of neighboring spheres within the system that is less than distance σ from the center of at least one other sphere within the cluster.

MC-generated configurations have been carried out to determine the probability distribution of a cluster of size N in equilibrium configuration. The transition is expected to be sharp in the limit of large N; however, the N-dependence is presently unknown. A FORTRAN subroutine CLUSTER for a hard sphere has been written to analyze large numbers of equilibrium configurations generated by standard Metropolis MC program.[3] The program calculates the probability distribution of clusters of size N. Figure 2 shows that at very low density, i.e., for an ideal gas, there are no clusters and $n_c/N = 1$. As the density increases, there are an ever-increasing number of pairs, then triplets, etc., and increasingly fairly large clusters, until eventually, there is just one cluster of size N that fill the whole box. At this point, the probability function $n_c/n = 1/N$; it goes to zero for large N.

The function $n_c(\rho)$ obtained from various data points taken from MC studies of the three system sizes investigated is shown in Figure 2. The first observation is rather unexpected: there is no obvious sharp phase transition point. There is no discontinuity in n_c/N, but there is a rather weak change in form in the density region around 0.07. These data give a clue to the percolation density, but are insufficient to determine it accurately. Also note from Figure 2 that $n_c(N,\rho)$ is surprisingly independent of N in the range 108, 864, and 6912. By contrast, the probability distribution for a cluster of size n is very strongly system size dependent. If we define a density-dependent %probability function $P(n,\rho)$) by

$$\%\mathrm{Pr}(n) = 100 \times n_c(n)n/N$$

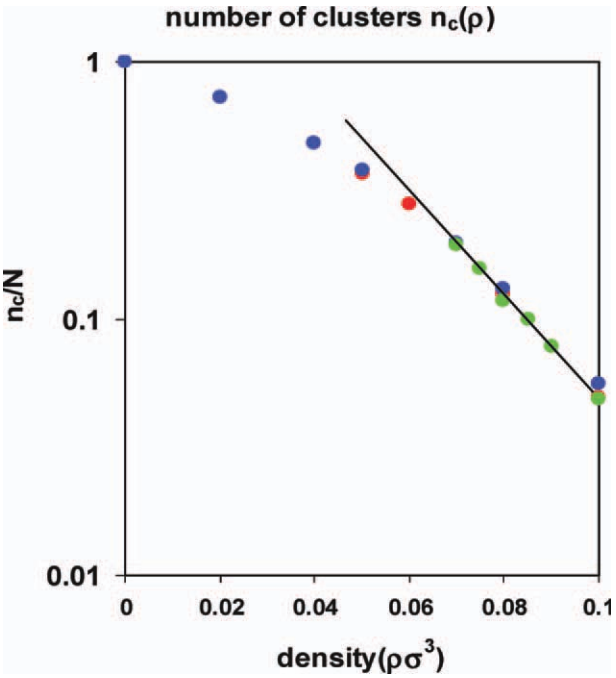

Figure 2. Density dependence of the total number of clusters divided by N: N = 108 (blue); N = 864 (red); N = 6912 (green).

The function is seen to change form in the vicinity of ρ_{pe}. [Color figure can be viewed in the online issue, which is available at wileyonlinelibrary.com.]

Multiplication by 100 is simply to avoid very small numbers on the log plots; the total probability normalizes to 100%, i.e., $\Sigma_n P_n = 100$.

Results for three densities of the system size $N = 108$ are shown in Figure 3. The data show that there is no sharp transition for such a small system and that the transition occurs over a rather wide range of density from 0.06 to 0.08. If we define the center point of the transition as the inflection to the first appearance of the second peak, it can be seen to occur at the density $\rho\sigma^3 = 0.068$.

For a system size of $N = 864$, clearer indications of a fairly sharp percolation transition can be seen from the cluster probability distributions (Figure 4). For densities 0.1 or greater, there are clusters of size of-the-order $O(N)$ that clearly span the whole system, coexisting with a few isolated very small breakaway single cluster, then dimers, etc. Now, the largest cluster to be found at the density 0.06 is very much less than N. The transition is still continuous but becomes sharper with larger N, and from the data in Figure 4, the saddle point appears to be midway between 0.07 and 0.075.

Further MC computations were then carried out to obtain the cluster distribution for a system size $N = 6912$, and the distribution is now beginning to show a sharper transition, but of course only an infinite size system will exhibit a truly sharp transition. From Figure 5 it can be seen that the density of saddle point is increasing with system size.

Plotting the saddle point ($\rho_{pe}(N)$ against $N^{1/3}$ gives a straight line that interpolates to the result ρ_{pe} ($N = \infty$) = 0.0785 with an estimated uncertainty of ± 0.01 (Figure 6).

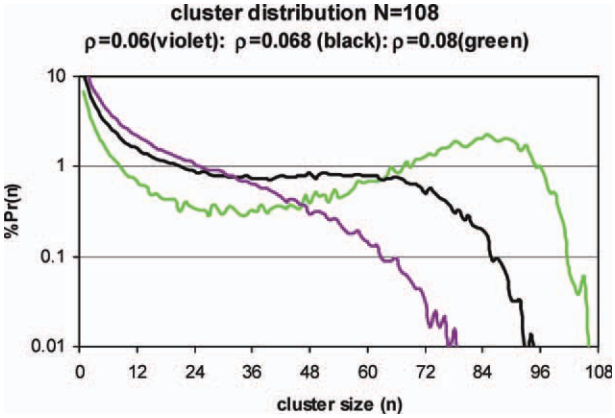

Figure 3. Normalized percentage probability of a sphere belonging to a cluster of size *N* for a system of 108 hard spheres with periodic boundary conditions for densities above (green) and below (violet) percolation, and the intermediate density (black) for which a "saddle node" can be regarded as the mid-point of the transition.

[Color figure can be viewed in the online issue, which is available at wileyonlinelibrary.com.]

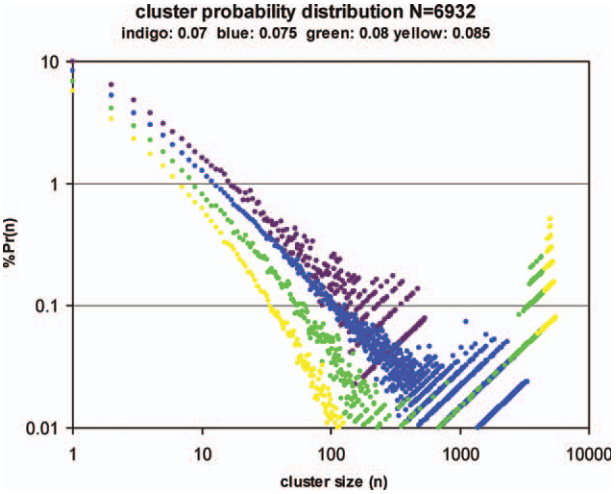

Figure 5. Normalized percentage probability of a sphere belonging to a cluster of size *N* for a system of 6912 hard spheres with periodic boundary conditions at a range of densities around the excluded volume percolation density (ρ_{pe}).

[Color figure can be viewed in the online issue, which is available at wileyonlinelibrary.com.]

This result is in agreement with the value obtained earlier from Heyes et al.,[15] assuming a very small margin of uncertainty in the value 0.771 derived earlier from their data. The earliest previous estimate of ρ_{pe} is given in the article by Kratky[11] (Eq. 18 in Ref. 11) as being in the range $0.076 < \rho_{pe}\sigma^3 < 0.084$ and was obtained from Ref. 12. The present result $\rho_{pe}\sigma^3 = 0.0785 \pm 0.01$ is also within the range of these earlier predictions.

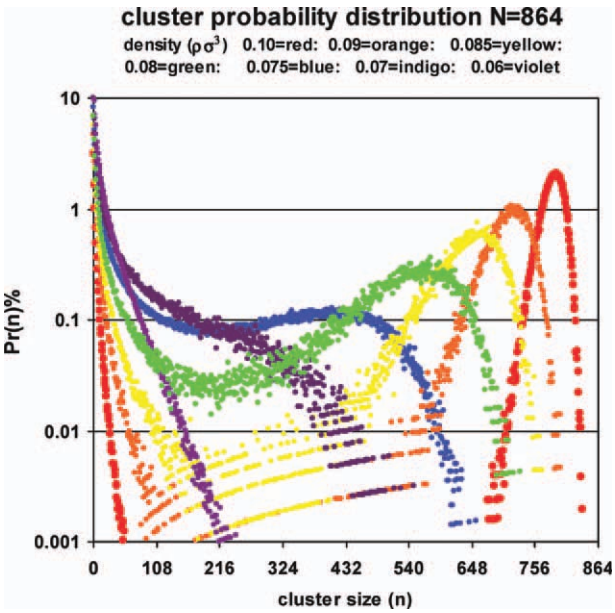

Figure 4. The normalized percentage probability of a sphere belonging to a cluster of size *N* for a system of 864 hard spheres with periodic boundary conditions for a range of densities around the excluded volume percolation density (ρ_{pe}).

[Color figure can be viewed in the online issue, which is available at wileyonlinelibrary.com.]

Radial Acceptance Function

Before investigating the available volume percolation and determining its density of occurrence, first note that both $<V_a>$ and its radial-resolved accessible volume function are directly obtainable from Metropolis MC calculation acceptance statistics. A radial acceptance function $u(r)$ can be defined as the probability of any sphere at position $r_{i,\mathrm{old}}$ in an equilibrium configuration, which is randomly moved a distance r to a site $r_{i,\mathrm{new}}$ that the trial site $r_{j,\mathrm{new}}$ does not fall within a radius σ of any other j-sphere, i.e., $r_{i,\mathrm{new}} - r_j > \sigma$ for all other $(N-1)$ spheres.

The radial acceptance function $u(r)$ is shown over the whole density range in Figure 7; $u(r)$ is unity at $r = 0$ and approaches a constant value at $r >> \sigma$.

A sphere site and an available cavity site in an equilibrium configuration have the same statistical properties.[9,13] For distances $r > \sigma$, $u(r)$ can equally be obtained by accumulation of the acceptance probability that a site any distance r_{ij} from any other sphere j is also an available cavity site. These statistics are also directly obtainable from conventional Metropolis MC method. For every trial move, a list of distances of the provisional $r_{i,\mathrm{new}}$ is saved and entered into an $\mathrm{acc}_j(r + \delta r)$ histogram only if the move is accepted; normalization of $\mathrm{acc}_j(r + \delta r)$ gives $u(r)$ for $r > \sigma$ according to

$$u(r) = \mathrm{acc}_j(r + \delta r)/(M\rho 4\pi r^2 \delta r) \tag{4}$$

where M is the total number of MC trial moves. This method of obtaining the radial acceptance function $u(r)$ is an accurate

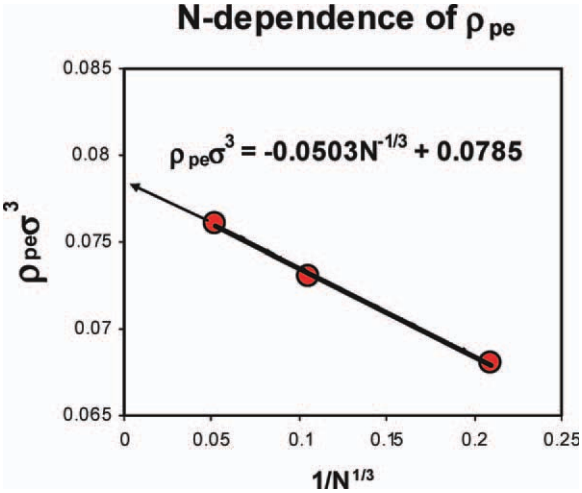

Figure 6. Determination of the excluded volume percolation transition density (ρ_{pe}) for the infinite *N* hard-sphere fluid by interpolation from the "saddle-point" probability nodes for the three finite systems: *N* = 6912, *N* = 864, and *N* = 108.

[Color figure can be viewed in the online issue, which is available at wileyonlinelibrary.com.]

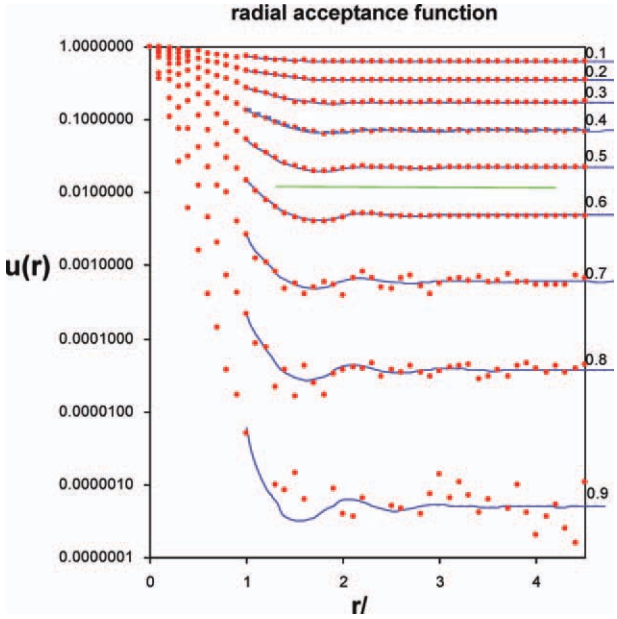

Figure 7. Radially resolved accessible-volume functions for range of fluid densities ($\rho\sigma^3$).

The red points are the acceptance ratio for moves of any sphere i and any distance r in an equilibrium configuration of large N. This gives $u(r)$ for all r. The blue lines are also the function $u(r)$ for $r > \sigma$ obtained by collecting the acceptance ratio of sphere i at any distance from all other j spheres. The horizontal green line indicates the position of the available volume percolation transition at ρ_{pa}. [Color figure can be viewed in the online issue, which is available at wileyonlinelibrary.com.]

means of obtaining chemical potentials without any additional computational effort in the MC calculation besides other equilibrium ensemble averages.

The radial acceptance function $u(r)$ can be factorized into the ensemble average available volume $<V_a>$ and the corresponding site–site distribution function; here, we simply retain the symbol $g(r)$ for r from 0 to ∞.

$$u(r)V = g(r)<V_a> \tag{5}$$

where $g(r)$ is the sphere cavity, site–site, normalized radial distribution function. Equation 5 can be regarded as a more formal definition of the radial acceptance function $u(r)$. For $r > \sigma$, $g(r)$ in Eq. 5 is the hard-sphere radial distribution function.

Relationships between $u(r)$ and thermodynamic properties are well established and have appeared in the literature before under various guises. Hoover and Poirier[4] were the first to consider the potential of mean force $\Psi(r)$ between two spheres separated by a distance r, given by

$$\Psi\,(r) = -kT\ \log_e g(r) \tag{6}$$

where $g(r)$ is continuous through the distance $r = \sigma$ and represents the potential of mean force of a pair of overlapping spheres . Hoover and Poirier found that at $r = 0$, i.e., when the two exclusion spheres effectively become one by occupying the same site without "seeing" each other, then

$$-\Psi(0) = \log_e(Q_{N-1}/Q_N) = -\mu/kT \tag{7}$$

which is the origin of Eq. 3. The reduced excess Helmoltz chemical potential of the hard-sphere fluid (μ) is defined relative to an ideal gas at the same temperature and volume. Equations 5 and 7 show that given the radial acceptance function $u(r)$ and the radial distribution function $g(r)$, the chemical potential may be obtained. For $r < \sigma$, however, particularly at $r = 0$, $g(0) = V/<V_a>$ may not so easy to obtain directly from MC computations.

Results for $r > \sigma$, however, obtained from MC calculations on $N = 864$ with periodic boundaries for $u(r)$ in Figure 7 show that acceptance function becomes constant at a few sphere diameters 2–3σ at low density and 3–4σ at high density, i.e., when $g(r)$ becomes unity. In this limit, we have

$$u(r \to 8) = <V_a>/V = \exp(-\mu/kT) = Q_{N+1}/Q_N, \tag{8}$$

and Widom's method[5,6] for the chemical potential is recovered. The whole range of r, however, can be used to improve the accuracy of thermodynamic properties using both $g(r)$ and $u(r)$ with Eqs. 5 and 8.

The radial acceptance function $u(r)$ has also been investigated from the statistical geometry aspect, in the range $r = 0$ to σ, by Speedy and Bowles.[13] They show that $u(0)$ and $u(\sigma)$ are related to each other through the relationship at $u(0)$ with the chemical potential and the relationship $g(\sigma)$ with the pressure. Knowledge of $u(r)$ over the whole range suffices to accurately determine all the thermodynamic state functions of the system given $g(0)$. [Note that $u(r)$ is the function "$n_0\ g_{00}(r)$" in Ref. 13].

Results for $u(r)$ in Figure 7 show no obvious change at the available volume percolation density ρ_{pa} though the slight structure for $r > \sigma$ maximum and minimum, which is the structure in $g(r)$ that disappears around $\rho\sigma^3 = 0.1$, i.e.,

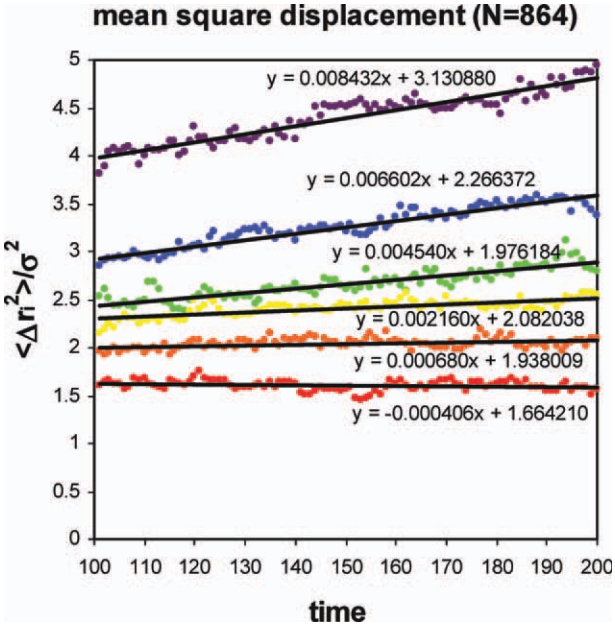

Figure 8. Mean squared displacement vs. time curves for diffusion of a single sphere in an otherwise static equilibrium configuration (N = 864) for states of the hard-sphere fluid in the vicinity of the accessible volume percolation transition (ρ_{pa}).

$\rho\sigma^3 = 0.55$ (red), 0.54 (orange), 0.53 (yellow), 0.52 (green), 0.51 (blue), 0.50 (violet). The dimension of time is $(m\sigma^2/k_BT)^{1/2}$. [Color figure can be viewed in the online issue, which is available at wileyonlinelibrary.com.]

in the vicinity of the excluded volume percolation density ρ_{pe}.

Available Volume Percolation

It is not a straightforward task to obtain the available volume percolation density just from the statistical averages of MC computations directly. To do so would require a selection of trial moves of sphere i only into the region of accessible volume (Hoover free volume v_{fi}) defined by its own cavity from the position at r_i, with all r_j kept fixed. The problem being the cavities that neighbor on sphere sites; accessible free volume v_f would have to be mapped and stored for each sphere could prove too onerous a task.

A much simpler way is to allow randomly selected spheres chosen from within equilibrium MC Metropolis-generated configuration, to diffuse freely and randomly given some kinetic energy, and hence to percolate the accessible volume if it is allowed to do so. Following this test procedure, the sphere is returned to its original site. If the kinetic energy is $(3/2)k_BT$ per sphere, the time scale is $(m\sigma^2/k_BT)$,$^{1/2}$ and a single-particle diffusion coefficient is then defined by the mean-squared displacement of many sample spheres (of the order $100 \times N$) over a very long time.

$$D_i = \frac{d<\Delta r_i^2>(t)}{6dt}$$

This definition of a single-particle diffusion coefficient is essentially Enskog's theoretical diffusion coefficient and

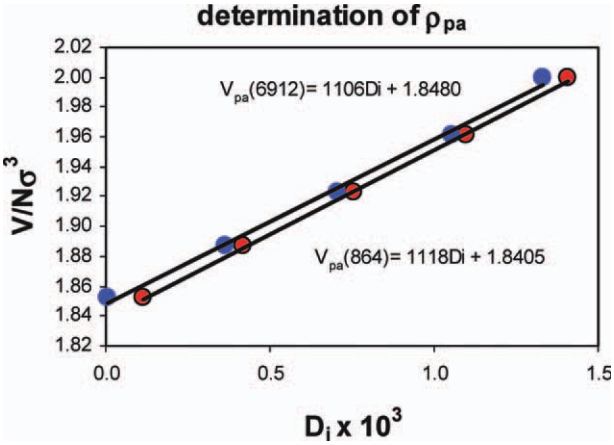

Figure 9. Single-particle diffusion coefficients (D_i) for two system sizes N = 864 (red) and N = 6912 (blue) in the vicinity of the percolation transition at ρ_{pa}.

[Color figure can be viewed in the online issue, which is available at wileyonlinelibrary.com.]

becomes equal to the low-density transport coefficient of self-diffusion in low-density gases where there are no correlations between successive collisions. These observations predict a discontinuity in the form of transport coefficients at the percolation transition ρ_{pa} (see previously for a system of hard parallel cubes).[10]

The results were sampled from equilibrium configurations using a FORTRAN subroutine HOLE, which selects a random sphere i, allocates a random velocity from a Gaussian distribution with mean = 0 and SD = 3, and solves the equations of motion of i with all $(N-1)$ j fixed in position, with frequent rerandomization to prevent numerical recurrence problems. Examples of displacement–time averages for the system size N = 864 are shown in Figure 8. Each curve was typically averaged over 100N, i.e., 86,400 trial diffusions, each trial diffusion lasting typically 50,000-100,000 collisions of sphere i in the diffusion time which was fixed at 200 $(m\sigma^2/k_BT)^{1/2}$. At the end of each cycle, i is returned to its original position so as not to affect the on-going MC equilibrium distribution.

The diffusion coefficients thus obtained for the different sized systems were then plotted against the volume of the system $(1/\rho\sigma^3)$; Figure 9) to determine the point of zero diffusion D_i, alternatively zero percolation of V_a for the different system sizes. The results for ρ_{pa} obtained for the two larger sizes N = 864 and N = 6912 are quite close.

The N-dependence of D_i can be seen in Figure 10, which includes results obtained for a small system of 108 spheres. The percolation transition density is found to decrease as $1/N$ for periodic systems. The interpolated value of $N = \infty$ is $\rho_{pa}\ \sigma^3 = 0.537$, with an estimated margin of uncertainty ± 0.005. This result is the first explicit determination of ρ_{pa} for spheres; however, there are previous estimates in the literature.[9,11,14] The first estimate was based on the observation of a change in non-Newtonian transport coefficients when the hard-sphere fluid is subjected to a shear stress field. The value that was suggested[14] is in the right range, but on the low side. The second estimate can be obtained from the

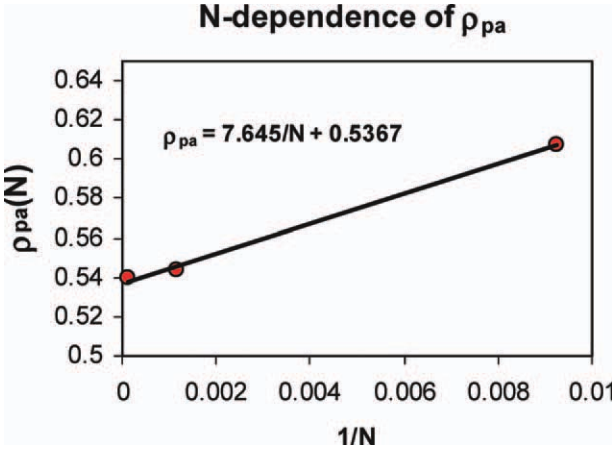

Figure 10. Dependence of the available volume percolation density (ρ_{pa}) on the size of the system.

The points shown are for systems of 108, 864, and 6952 all with periodic boundary conditions. [Color figure can be viewed in the online issue, which is available at wileyonlinelibrary.com.]

point at which Speedy's high-density equation-of-state, based on the distribution of holes at densities above ρ_{pa}, diverges. Speedy's estimated range of $\rho_{pa}\ \sigma^3 = 0.44 \pm 0.08$ is also just on the low side.[9,11]

Closed-Virial Equation-of-State

Very recently, it has been found[16] that a closed-virial equation-of-state for the $D = 2$ hard disk fluid begins to deviate from the thermodynamic pressure at or near the 2-D-percolation density $\rho_{pa}\sigma^2 = \rho_{pe}\sigma^2 = 0.4$ determined by Hoover et al.[8] Similar closed-virial equations-of-state for the hard-sphere fluid,[17,18] however, have been proposed and found to be equally accurate to 6-figure precision. However, the deviation from the thermodynamic pressures in the higher density range have not yet been scrutinized for errors from within the MD data and virial coefficient uncertainties. The 3-D virial equation has been shown to diverge at or below the freezing density. Now that we have accurate values of the percolation densities, we can test the speculative predictions of 23 years ago[10,11,14] that the hard-sphere percolation transition may be a higher-order thermodynamic transition.

The most accurate recommended values for all the known virial coefficients for hard spheres were taken directly from the study of Clisby and McCoy,[19] in which their values of b_n correspond to the virial expansion as given in Eqs. 2 or 3. Inspection of incremental values of successive virial coefficients, plotted (Figure 11) in powers of density relative to crystal close packing, shows that beyond $(B_8 - B_7)$, the increment decrease varies exponentially according to

$$B_n - B_{(n-1)} = A_0 + A\ \exp(-n) \tag{9}$$

The constant A can be obtained from $B_m - B_{m-1}$ and can be used to predict all higher values B_n from $m + 1$ to infinity, thereby effecting an analytic closure to the virial expansion.

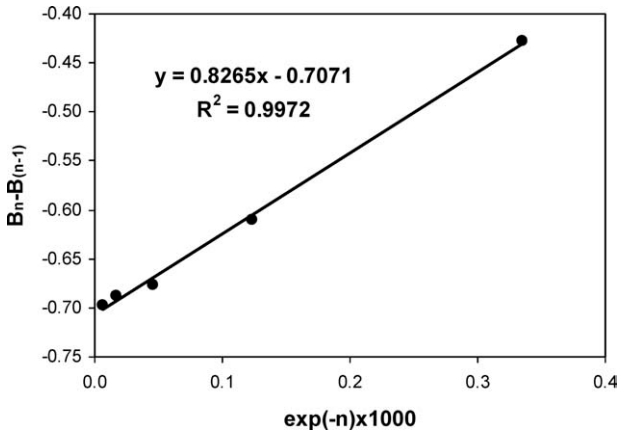

Figure 11. Difference between successive virial coefficients (B_n) from $n = 12$ to $n = 8$ in the expansion in powers of density relative to close packing.

The difference $B_n - B_{(n-1)}$ decreases as $\exp(-n)$ and approaches the constant $-1/\sqrt{2}$ when $n \to \infty$.

When the two Kolafa-Lablik-Malijeski (KLM)-predicted[20,21] virial coefficients B_{11} and B_{12} are included in the extrapolation to $n \to \infty$ (Figure 11), the value of A_0 is empirically found to be the reduced close-packed volume per sphere $-1/\sqrt{2}$ as noted previously [12,13] to 4-figure precision. The constant A can then be obtained from the known virial coefficients. This interpolation of all the known virial coefficients suggests that as the limiting value of $B_n - B_{n-1}$ is negative, the virial coefficients will eventually become negative and the corresponding virial equation-of-state will be continuous in all its derivatives, eventually showing a negative pressure, with the first pole at ρ_0. Equation 9 predicts a first negative coefficient at B_{19}.

The virial equation-of-state for hard spheres then takes the form

$$Z = 1 + \sum_{n=2}^{m} B_n\ \rho*^{(n-1)} + \sum_{n=m+1}^{\infty} (B_m + A_0 + A\ e^{-(m+1)})\rho*^{(n-1)} \tag{10}$$

Each term of this summation can be closed separately[12,13] to obtain an equation-of-state that enables the closure for any known value of n greater or equal to $m = 8$. When the constant A defined in Eq. 9 is replaced by the highest used virial coefficients $(B_m - B_{m-1} - A_0)$, we obtain

$$Z = 1 + \sum_{n=2}^{m} B_n\ \rho*^{(n-1)} + B_m \frac{\rho*^m}{(1-\rho*)} + A_0 \frac{\rho*^m}{(1-\rho*)^2} + (B_m - B_{(m-1)} - A_0) \frac{\rho*^m}{(1-\rho*)(e-\rho*)} \tag{11}$$

The last term is merely a very small correction for finite m that disappears for large m. It would appear from the data in Figure 1 and Table 1 that $m = 12$ is sufficiently large for 6-figure accuracy up to high density. If we now close at $m = 12$ and put

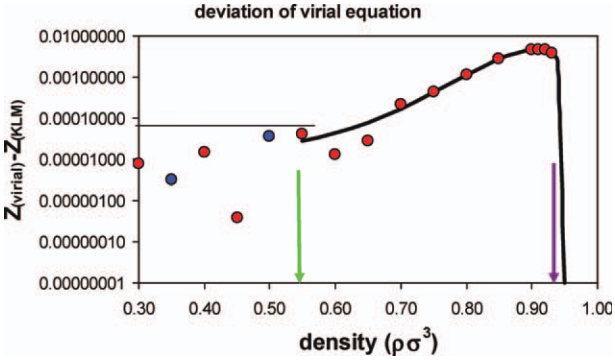

Figure 12. Deviation of closed-virial equation-of-state (Eq. 9: $m = 12$) and thermodynamic pressures obtained from MD simulations by Kolafa et al.[20]

The horizontal line at 0.00004 is the uncertainty limit in the KLM MD Z-values; blue circles are the moduli of negative values; the percolation transition density is indicated by the vertical green arrow; and the fluid freezing density[21] is shown by the purple arrow. [Color figure can be viewed in the online issue, which is available at wileyonlinelibrary.com.]

$A_0 = -1/\sqrt{2}$, Eq. 4 reduces to the original WC1[18] equation[18,19] with the constant A_0 empirically fixed at $-V_0$

$$Z = 1 + \sum_{n=2}^{m} B_n \, \rho*^{(n-1)} + B_m \frac{\rho*^{m}}{(1-\rho*)} - \frac{\rho*^{m}}{\sqrt{2}(1-\rho*)^2} \quad (12)$$

with no other parameters save the virial coefficients up to $m = 12$, an equation-of-state that reproduces the Pade approximant equation of Clisby and McCoy[19] over the whole range of densities with 6-figure accuracy.

The pressure given by the closed-virial equation (Eq. 12) can be compared with the thermodynamic pressure from MD computations in the vicinity of melting. In Figure 12, we compare with the KLM data[20,21] up to the freezing density.[22] The comparison shows that the deviation is real and is beginning at a much lower density. This implores the question: "where is the first deviation and what is the underlying science?" The virial expansion becomes exact at very low density, with convergence up to $\rho\sigma^2 = 0.025$ having been rigorously proven by Lebowitz and Penrose.[23] As the virial equation is continuous in all its derivatives, if the thermodynamic pressure deviates, it must be signaled by a thermodynamic phase transition of second or higher order.

The differences between the closed-virial equation and the thermodynamic MD pressures from the literature are shown in Figure 12. The comparison shows that the deviation is originating at or below the percolation density (ρ_{pa}).

A close inspection of the deviation in Figure 12 suggests that the virial equation-of-state begins to deviate from the thermodynamic pressure obtained for 6-figure accuracy from MD simulations at a density above or below the available volume percolation density ρ_{pa}. This deviation is statistically significant and it would appear from the forgoing analyses that it cannot be explained by uncertainties in the thermodynamic pressures or errors in the known virial coefficients, or any combination of both. We cannot say, however, within the uncertainties that the deviation does not begin at the lower percolation transition density (ρ_{pe}).

Conclusions

The current analysis of the available volume and its percolation transitions for the simple hard-sphere model should be applicable to all hard-core models. The radial acceptance function $u(r)$ for the chemical potential, for example, becomes a function of the angles of displacement $u(r,\phi,\varphi)$ and also of $g(r,\phi,\varphi)$, and therefore, Eq. 5 and all the definitions for the available volume and chemical potential are still valid.[24] The use of the radial acceptance function $u(r)$ as a means to chemical potentials from MC acceptance statistics is also applicable to nonspherical systems.

It now seems likely that all hard-core models will exhibit a percolation transition of some kind, beyond which the virial expansion will not represent the thermodynamic pressure. This means that the hard-sphere fluid has associated with its percolation transition ρ_{pa} by both a gas-like phase for $r < \rho_{pa}$ and a liquid-like phase for $\rho > \rho_{pa}$. At present, little is known about the thermodynamic Ehrenfest order of this phase transition, except that it is not first. A third-order phase transition seems the most likely because at the percolation transition, there is likely to be a change in the nature of the number density fluctuations, which are related to the second density derivative of the chemical potential. This is now a topic for future research.

Perhaps of greater interest is what happens to the percolation transition when an attractive perturbation is added to the hard-sphere pressure, which now requires two different equations-of-state to represent the whole fluid range. We have a highly accurate virial equation for $\rho < \rho_{pa}$, but the best we can do at present on the high-density side is the equation-of-state of Speedy[9] or something similar; however, it is going to be difficult to make the connection without more detailed knowledge of the nature of the percolation transition than we have at present.

There is now a real prospect, however, after 100 years since van der Waals, of obtaining a theoretical equation-of-state of gases and liquids, in the spirit of van der Waals, but for which the condensation transition is not simply contrived by fitting to the node of a cubic equation. There is presently a number of theoretical activities[25] involved in predicting the properties of square-well fluids using approximations that have their origins in the ad hoc truncation or neglect of various terms in the Mayer cluster expansion (Eq. 2).

Here, we make the simple observation that a square-well perturbation will have a different effect on both sides of the percolation transition; however, now we do not need to arbitrarily drop terms by guessing.[3] The cluster expansion itself is not applicable above ρ_{pa}. As the perturbation gets stronger or, equivalently, as the temperature is reduced, the line of the percolation transition density can only come to an end at a critical point. Beyond this, the total chemical potential of two separate phases becomes less than their would-be mixture at the percolation density. Hence, it is tempting to speculate even further that the extrapolation of ρ_{pa} into the two-phase region will become the "law of rectilinear diameters" that bisects gas and liquid densities as a function of temperature.

Acknowledgments

The author thanks the University of Delaware for a Visiting Professorship in the Centre for Molecular and Engineering Thermodynamics for financial support, and in particular, the author's host at the University of Delaware, Prof. Stanley I. Sandler for his support and encouragement for this research.

Literature Cited

1. van der Waals JD. Simple deduction of the characteristic equation for substances with extended and composite molecules. *Kon Ned Akad Wet Amst Proc Sec Sci*. 1899;1:138–143.
2. Mayer JE, Mayer MG. *Statistical Mechanics*. New York: Wiley, 1940.
3. Hansen J-P, McDonald IR. *Theory of Simple Liquids*, 4th ed. Oxford: Academic Press, 2008.
4. Hoover WG, Poirier JC. Determination of virial coefficients from potential of mean force. *J Chem Phys*. 1962;37:1041–1042.
5. Widom B. Some topics in the theory of fluids. *J Chem Phys*. 1963;39:2808–2812.
6. Adams DJ. Chemical potential of hard-sphere fluids by Monte Carlo methods. *Mol Phys*. 1974;28:1241–1252.
7. Stauffer D. *Introduction to Percolation Theory*. London: Taylor and Francis, 1985.
8. Hoover WG, Hoover NE, Hanson K. Exact hard-disk free volumes. *J Chem Phys*. 1979;70:1837–1844.
9. Speedy RJ. Cavities and free volumes in hard-disc and hard-sphere systems. *J Chem Soc Faraday Trans 2*. 1981;77:329–335.
10. van Swol F, Woodcock LV. Percolation transition in the parallel hard cube model fluid. *Mol Simul*. 1987;1:95–108.
11. Kratky KW. Is the percolation transition of hard spheres a thermodynamic phase transition. *J Stat Phys*. 1988;52(5/6):1413–1421.
12. Bug ALR, Safran SA, Grest GS, Webman I. Do interactions raise or lower a percolation threshold? *Phys Rev Lett*. 1985;55:1896–1899.
13. Speedy RJ, Bowles RK. Statistical geometry and cavity correlations in the hard-sphere fluid. *Collect Czech Chem Commun A*. 2008;73:344–357.
14. Woodcock LV. Developments in non-Newtonian rheology. *Lect Notes Phys*. 1987;277:113–123.
15. Heyes DM, Cass M, Branka AC. Percolation threshold of hard-sphere fluids in between the soft-core and hard-core limits. *Mol Phys*. 2006;104:3137–3146.
16. Beris A, Woodcock LV. Closed virial equation-of-state for the hard-disk fluid, LANL ar.Xiv. 2010:1008.3872 [pdf].
17. Woodcock LV. Virial equation for hard spheres, LANL ar.Xiv. 2008: 0804.0679 [pdf].
18. Bannerman M, Lue L, Woodcock LV. Thermodynamic pressures for hard spheres and closed virial equation-of-state. *J Chem Phys*. 2010;132:084507.
19. Clisby N, McCoy BN. Ninth and tenth virial coefficients for hard hyper-spheres in D-dimensions. *J Stat Phys*. 2006;122:15–57.
20. Kolafa J, Labik S, Malijevsky A. Molecular dynamics and equations-of-state for hard spheres and disks. *Phys Chem Chem Phys*. 2004;6:2335–2345.
21. Labík S, Kolafa J, Malijevský A. Virial coefficients of hard spheres and hard disks up to the ninth. *Phys Rev E*. 2005;71:021105.
22. Hoover WG, Ree FH. Melting transition and communal entropy for hard spheres. *J Chem Phys*. 1968;49:3609–3618.
23. Lebowitz J, Penrose O. Convergence of virial expansions. *J Math Phys*. 1964;5:841–847.
24. Gay SC, Rainwater JC, Beale PD. Two-dimensional hard dumbbells. II. Pressure in terms of free volumes and surfaces. *J Chem Phys*. 2000;112:9849–9860.
25. Scholl-Passinger E, Benavides AL, Castaneda-Priego R. Vapor-liquid equilibrium and critical behavior of the square-well fluid of variable range: a theoretical study. *J Chem Phys*. 2005;123:234513.

Manuscript received Dec. 2, 2010, revision received Feb. 27, 2011, and final revision received Apr. 22, 2011.